CERN-TH/99-170
MADPH-99-1124
hep-ph/9907365

Dark Matter Abundance and Electroweak Baryogenesis in the CMSSM

Sacha Davidson
CERN Theory Division, CH-1211 Genève 23, Switzerland

Toby Falk
Department of Physics, University of Wisconsin, Madison, WI 53706, USA

Marta Losada[1]
CERN Theory Division, CH-1211 Genève 23, Switzerland

Abstract

The Minimal Supersymmetric Standard Model has a candidate dark matter particle in its spectrum, and may be able to generate the baryon asymmetry of the Universe (BAU) at the electroweak phase transition. In the Constrained MSSM, we find the area of parameter space which is allowed by accelerator and precision tests, which produces a relic dark matter abundance in the observationally favored window $0.1 \lesssim \Omega h^2 \lesssim 0.3$, and where baryon plus lepton number violating processes are out of equilibrium after the electroweak phase transition.

June 1999

[1]On leave of absence from the Universidad Antonio Nariño, Santa Fe de Bogotá, COLOMBIA.

1 Introduction

Two intriguing features of the Minimal Supersymmetric Standard Model (MSSM) from a cosmological perspective are that the Lightest Supersymmetric Particle (LSP) is a stable dark matter [1] candidate, and that electroweak baryogenesis[2] might be possible for certain parameter choices. Moreover, large regions of the baryogenesis parameter space should be accessible to the presently running LEP200.

The stability of the LSP is ensured by R-parity, which is often imposed on supersymmetric models to avoid rapid proton decay and to satisfy other phenomenological bounds [3]. The $R-$parity of a particle is $(-1)^{3B+L+2S}$, where S is its spin. Standard Model particles are even under $R-$parity, and supersymmetric partners are odd, so the LSP cannot decay. The LSP freezes out of chemical equilibrium in the early universe, enhancing its relic abundance, and its mass density is often large enough to be cosmologically significant, particularly when the LSP is a gaugino-type neutralino. It is an appealing feature of supersymmetry that it naturally provides a stable dark matter candidate, with a relic density in the cosmologically preferred range $0.1 \lesssim \Omega h^2 \lesssim 0.3$, discussed below.

A second cosmologically interesting feature of supersymmetric models is that it may be possible to generate the baryon asymmetry at the Electroweak Phase Transition (EWPT) [2]. The three ingredients required for baryogenesis, Baryon number violation, C and CP violation and out-of-equilibrium dynamics [4], are present in the Standard Model (SM) at the EWPT. However, generating the observed baryon asymmetry at the EWPT is not possible in the Standard Model [5, 6] because the non-perturbative Baryon plus Lepton ($B+L$) number violating sphaleron processes [7] remain in equilibrium after the phase transition and will wash out any asymmetry in $B+L$ present at that time [8]. A necessary condition for electroweak baryogenesis is that these processes be out of equilibrium after the $B+L$ asymmetry is generated at the phase transition. This requirement translates into having a sufficiently strong first order electroweak phase transition at finite temperature and is satisfied for various extensions of the SM [9], including the MSSM with a light stop [10, 11, 12].

There has been much work on constraining supersymmetric models using the combined bounds from accelerator experiments and the cosmological relic abundance [13]. The area of SUSY parameter space in which electroweak baryogenesis could work (no $B+L$ violation after the transition) has also been studied in some detail [14, 11, 10]. The purpose of this paper is to combine these two cosmologically interesting features of supersymmetry. In the Constrained MSSM (CMSSM), where the soft SUSY breaking parameters $m_0, m_{1/2}$ and A are universal at the GUT scale, we find the area of parameter space consistent with present LEP bounds on sparticle masses, with the measured $b \to s\gamma$ branching ratio, and with precision tests of the ρ parameter, where it would be possible to preserve a baryon asymmetry generated at the electroweak phase transition, and where the relic density of LSPs satisfies $0.1 \lesssim \Omega h^2 \lesssim 0.3$.

It is interesting that there remains a finite area of CMSSM parameter space satisfying all the constraints, although the area is not very large (see Figs. 2-4). Moreover, most of the area is accessible to LEP200; Higgs searches should tell us if we live in this area of CMSSM parameter space.

2 Cosmological and Experimental Constraints

A prerequisite for successful electroweak baryogenesis is that any asymmetry created at the phase transition not be washed out afterwards. This means that the $B+L$ violating electroweak processes,

which are suppressed by a factor of order $e^{-4\pi\phi/(gT)}$ after the transition, must be out of equilibrium. This will be the case if [15]

$$\frac{\phi(T_c)}{T_c} \gtrsim 1, \tag{1}$$

where $\phi(T_c)$ is the vacuum expectation value (vev) of the Higgs in the broken minimum of the Higgs potential at the temperature T_c where the two minima are degenerate.

The jump in the Higgs vev can be calculated in various ways. One can compute loop corrections in perturbation theory to the finite temperature effective potential $V_{eff}(\phi, T)$. The generic form of the effective potential potential is

$$V_{eff}(\phi, T) = \frac{\gamma}{2}T^2\phi^2\left[1 - B\ln\left(\frac{\phi}{T}\right)\right] - \frac{m^2}{2}\phi^2 - ET\phi^3 + \frac{\lambda}{2}\phi^4, \tag{2}$$

in which case, at the critical temperature,

$$\frac{\phi(T_c)}{T_c} = \frac{E}{2\lambda} + \frac{1}{2}\sqrt{\frac{E^2}{\lambda^2} + \frac{2\gamma B}{\lambda}} \simeq \frac{E}{\lambda}\left(1 + \frac{\lambda\gamma B}{E^2}\right) \quad . \tag{3}$$

For a given model, the parameters γ, E, λ and B are calculable functions of the zero temperature coupling constants. The B-term is an approximation aimed to model two-loop QCD corrections in the MSSM [16]. In this perturbative approach, the ratio of the Higgs vev to the temperature is increased by having a larger cubic term, a larger B, and a smaller quartic coupling λ. At zero-temperature, λ is related to the mass of the Higgs particle. At tree level in the SM, $m_H^2 = 4\lambda\phi^2$, so small λ corresponds to small Higgs mass. When quantum corrections are included, the relationship becomes less simple, but the condition (1) still translates into an upper bound on the Higgs mass.

The cubic term arises in the high temperature expansion of the one-loop contribution to the effective potential from bosons which couple to the Higgs vev [17]. There is a term $-(m_b^2)^{3/2}T/(12\pi)$, which contains a term $\phi^3 T$ for a boson mass $m_b^2 = m^2 + c_1\phi^2 + c_2T^2$. If m^2 and c_2 are small enough, the effective potential is approximately of the form (2). The one-loop contribution to E from the W and Z bosons is $(2g^3 + [\sqrt{g^2 + g'^2}]^3)/(32\pi)$ [18], but this is not large enough to satisfy equation (1) for experimentally allowed values of the Higgs mass (which determines λ) in the SM.

In extensions of the Standard Model, additional particles in the thermal bath contribute to the effective potential. Of particular interest are the new bosons which couple strongly to the Higgs field and can modify the contributions to the cubic term in the potential. In the MSSM [2], a light squark would contribute a term $\sim h_q^3 \sin^3\beta/(4\pi\sqrt{2})$ to E, which would be substantial for the top Yukawa coupling h_t. To see this, consider the finite temperature mass matrix for the doublet and singlet stops:

$$\begin{bmatrix} m_{Q_3}^2 + \frac{1}{2}h_t^2\sin^2\beta\ \phi^2 + \frac{1}{8}g^2\cos 2\beta\ \phi^2 + \mathcal{O}(T^2) & -\frac{1}{\sqrt{2}}h_t\phi\sin\beta(A + \mu\cot\beta) \\ -\frac{1}{\sqrt{2}}h_t\phi\sin\beta(A + \mu\cot\beta) & m_{U_3}^2 + \frac{1}{2}h_t^2\sin^2\beta\ \phi^2 + \mathcal{O}(T^2) \end{bmatrix} \tag{4}$$

where we normalize $m_W = g\phi/2$, we neglect the $U(1)$ coupling, and $m_{Q_3}(m_{U_3})$ is the third generation doublet (singlet) squark soft SUSY-breaking mass. If we neglect doublet-singlet mixing, then $(m_{\tilde{t}_R}^2)^{3/2} = (m_{\tilde{U}_3}^2 + h_t^2\sin^2\beta\ \phi^2/2 + 4g_s^2T^2/9 + \frac{1}{6}(1+\sin^2\beta)h_t^2T^2)^{3/2}$ is of order $h_t^3\phi^3$, if $m_{\tilde{U}_3}^2$ is negative

[2]For large values of m_A, the lightest Higgs quartic self-coupling is fixed at tree-level to be $\lambda = \frac{g^2}{8}\cos^2 2\beta$.

and cancels the finite temperature contributions. We cannot make the other stop light, because two light stops increase the ρ parameter beyond its measured value. In the MSSM at two loops, the light singlet stop contribution to E is sufficient to satisfy equation (1).

A drawback to the perturbative evaluation of the effective potential is that it has infra-red divergences as the Higgs vev ϕ approaches zero. These are due to bosonic modes whose only mass in the perturbative calculation is proportional to ϕ. Resummation is then employed to deal with these divergences. The net effect in the case of the Standard Model is to reduce the contribution from the gauge bosons to the cubic term, thus weakening the strength of the phase transition. An alternative way to compute the ratio (1) is using Monte Carlo 3-d lattice simulations via dimensional reduction [19]. In dimensional reduction an effective 3-d theory is constructed perturbatively integrating out all the massive modes. The characteristics of the phase transition can then be determined by simulating on the lattice the remaining 3-dimensional theory of massless bosonic modes. The strength of the lattice simulations is that they can constrain a whole class of models which are described by the same effective 3-d theory containing a single light scalar at the phase transition.

Simulations have also been done for the case where there is a colored $SU(2)$ singlet among the light/massless modes at $\phi = 0$ [11]. This corresponds to the light RH stop scenario that could make the phase transition strong enough in the MSSM. The area of MSSM parameter space where the EWPT is strong enough was found in the lattice analysis to be larger than the area found in perturbation theory. This means that calculating $\phi(T_c)/T_c$ from the perturbative effective potential is conservative, so this is what we will do. We construct the effective potential via dimensional reduction.

The effective 3D theory constructed with dimensional reduction reproduces the perturbative 4D effective potential results. The 3-D theory naturally incorporates the effects of resummation and some higher order corrections. We use the results given in ref. [12] for the two-loop finite-temperature effective potential of the MSSM with a light stop. It assumes that the b-quark Yukawa coupling is small (this restricts the value of $\tan\beta \lesssim 15$), and is calculated in the limit where all the supersymmetric particles are heavy ($\sim$ TeV) except for the stops[3]. The heavier stop is included in the high-temperature expansion, rather than as a TeV-mass particle, because the areas of CMSSM parameter space we are interested in typically predict a heavy stop mass $\gtrsim 300$ GeV.

The conclusions of the two-loop perturbative analysis for the MSSM [20, 10, 12] are that the sphaleron transitions are suppressed when the stop and Higgs bosons are light enough. However, the maximum possible values of $m_{\tilde{t}_2}$ (the light stop mass), and m_h for which (1) is satisfied depend also on the trilinear terms and on $\tan\beta$. The presence of $h_t\mu H_1^\dagger Q_3 U_3^c + h_t A H_2 Q_3 U_3^c$ in the potential weakens the strength of the phase transition, because these terms reduce the contribution of the light stop $\tilde{t}_2$ to E (that is, E decreases for fixed $m_{\tilde{t}_2}$ as $(A + \mu\cot\beta)$ increases), it makes the Higgs heavier and increases the value of T_c. These undesirable effects of trilinears on the survival of the BAU can be partially compensated by decreasing the singlet stop soft mass $m^2_{U_3}$. So if for fixed $(A + \mu\cot\beta)$ one can independently decrease $m^2_{U_3}$, one can find a combination of m_h, $m_{\tilde{t}_2}$, $(A + \mu\cot\beta)$ (and $\tan\beta$) such that the phase transition is strong enough. Of course, there is a lower bound on $m_{\tilde{t}_2}$ from

[3]We include scalar boson doublets and singlets with masses $m \lesssim 2\pi T$, such that the high-temperature expansion is valid. Neglecting the contributions from all other sfermions and other supersymmetric particles which do not couple strongly to the Higgs boson is a good approximation. The Higgsino does couple through the top Yukawa but as it is a fermion it does not strongly affect the strength of the phase transition.

direct searches, which puts an upper bound on the amount of mixing in the stop sector with which the BAU can be preserved. However, as we shall see, it is difficult in the CMSSM to make $m^2_{U_3}$ at the weak scale smaller for fixed $(A + \mu \cot \beta)$, because it is the A parameter that one is using to run the soft mass $m^2_{U_3}$ negative (see eqn. 5), so the $m^2_{U_3}$ and $(A + \mu \cot \beta)$ are not independent. In the CMSSM it is therefore not trivial to produce a light stop with little left-right mixing.

The physical masses m_h and $m_{\tilde{t}_2}$ for which the phase transition is sufficiently first order depend mildly on $\tan \beta$. The Higgs mass increases with $\tan \beta$, so for larger $\tan \beta$ one needs a lighter stop. For fixed $\tan \beta$, the zero stop mixing case $(A+\mu \cot \beta) = 0$ provides the least stringent bound on $m_{\tilde{t}_2}$, which is of order $m_{\tilde{t}_2} < m_t$ (as discussed following eqn 4). The largest possible value of the Higgs mass m_h is determined by the largest allowed value of the mixing parameter; for $m_Q = 300$ GeV it is $m_h \lesssim 105$ GeV. This is because the stop loop contribution to m_h increases with stop mixing.

A two-stage phase transition can appear at finite temperature in certain regions of parameter space. The fact that the stop is light allows the possibility of tunneling into a color and charge breaking minimum [20, 10, 12, 21], from which the Universe would subsequently undergo a transition to the $SU(2)$ broken minimum. The recent analysis of ref. [21] shows that the second phase transition may not take place, thus giving stronger constraints on the allowed parameter space. This gives a lower bound on the stop mass for every set of values of the mixing parameter and $\tan \beta$. This lower bound is larger than the direct experimental search limit on $m_{\tilde{t}_2}$. In the present paper we do not include this constraint.

We are interested in an area of CMSSM parameter space where the Higgs is light and the singlet stop soft mass is negative. The one-loop Renormalization Group Equation (RGE) for this stop mass is [22]

$$\frac{dm^2_{\tilde{U}_3}}{dt} = \frac{16}{3}\frac{\alpha_3}{4\pi}M_3^2 - 2\frac{h_t^2}{16\pi^2}(m^2_{Q_3} + m^2_{U_3} + m^2_{H_2} + A_t^2) \tag{5}$$

where $t = ln(m^2_{GUT}/Q^2)$, M_3 is the gluino mass, α_3 is the strong coupling, H_2 is the Higgs that couples to the top quarks, and we have neglected contributions proportional to $\alpha_1 M_1^2$. One can see that the gluino runs the stop mass up as the soft masses are evolved down from the GUT scale, but a sufficiently large $|A_0|$ at the GUT scale will run $m^2_{\tilde{U}_3} \lesssim 0$ near the electroweak scale. From approximate analytic solutions to the one-loop RGEs [23], one finds that $m^2_{\tilde{U}_3} \sim 0$ for $|A_0| \sim 11|m_{1/2}|$.

In addition to the restrictions imposed on the CMSSM by the preservation of the baryon asymmetry, we consider both experimental constraints from LEP particle searches [24] and cosmological constraints on the relic density of the lightest supersymmetric particle. Over much of the CMSSM parameter space, the LSP is a bino $\widetilde{B}$. For a gaugino-type neutralino, annihilation in the early universe occurs primarily via sfermion exchange into fermion pairs, and in particular into lepton pairs in the CMSSM. Since the sleptons become more massive with m_0, the neutralino annihilation rate decreases, and the neutralino relic abundance increases as m_0 is raised, leading to an effective upper bound on the scalar mass parameter. An exception occurs when the neutralino mass is close to half the Higgs or Z mass, so that s-channel annihilation on the Higgs or Z pole can dominate, and the relic abundance satisfies $\Omega_{\widetilde{\chi}} h^2 \leq 0.3$ independent of m_0.

In Fig. 1, the cosmological and experimental bounds are displayed in the $(m_0, m_{1/2})$ plane for the representative choice $\tan \beta = 6$, $A_0 = 0$, and $\mu < 0$. The light shading denotes the region where the neutralino relic density lies in the cosmologically preferred range $0.1 \leq \Omega_{\widetilde{\chi}} h^2 \leq 0.3$ and is fairly insensitive to $\tan \beta$ for the small to moderate values of $\tan \beta$ which are relevant. The upper

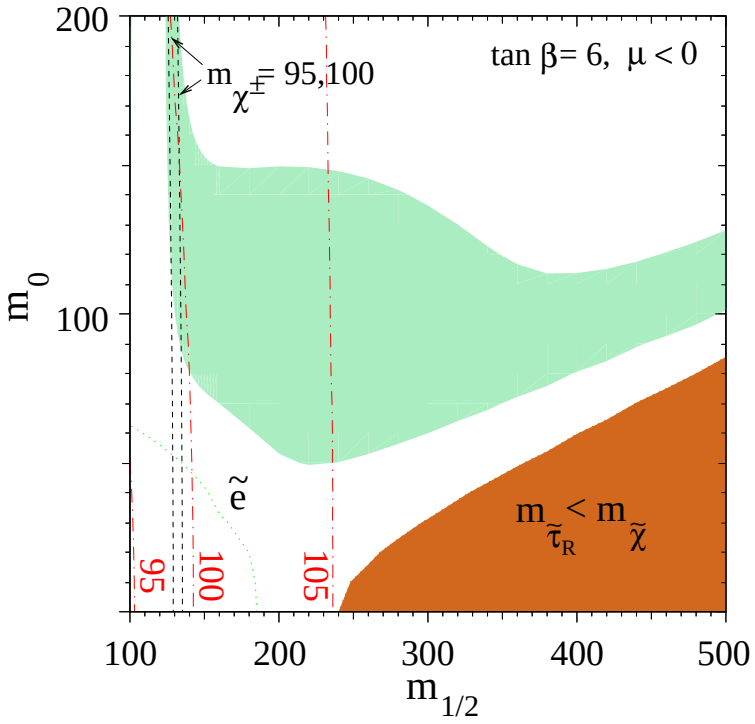

Figure 1: *The light-shaded area is the cosmologically preferred region with* $0.1 \leq \Omega_{\tilde{\chi}} h^2 \leq 0.3$. *In the dark shaded region, the LSP is the* $\tilde{\tau}_R$, *leading to an unacceptable abundance of charged dark matter. Also shown are the isomass contours* $m_{\chi^\pm} = 95, 100$ *GeV (dashed) and* $m_h = 95, 100$ *GeV (dot-dashed), as well as an indication of the slepton bound (dotted line) from LEP [24].*

bound (which provides the boundary at large m_0 and $m_{1/2}$) arises from the requirement that the universe be older than $t_U > 12$ Gyr. The lower limit requires that the relic neutralinos contribute appreciably to the dark matter of the universe and is more of a preference that a bound, in contrast to the upper limit. The narrow chimney which extends to large m_0 at $m_{1/2} \sim 120\,\mathrm{GeV}$ is due to s-channel annihilation on the Higgs and Z poles. In the dark shaded region of Fig. 1, the lightest supersymmetric particle is the stau $\tilde{\tau}_R$, which is forbidden by the stringent limits on charged dark matter [25]. The shaded region bends away from the line $m_{\tilde{\tau}_R} = m_{\tilde{\chi}}$ due to stau annihilation and stau-neutralino coannihilation, which significantly deplete the neutralino relic abundance for small neutralino-stau mass splittings [26]. We'll see below that preserving the baryon asymmetry requires $m_{1/2} \lesssim 300\,\mathrm{GeV}$, and so from Fig. 1, $\Omega_{\tilde{\chi}} h^2 \leq 0.3$ necessitates $m_0 \lesssim 170\,\mathrm{GeV}$, outside of the pole region.

The experimental bound on the chargino mass in the CMSSM saturates the kinematic limit of ~ 95 GeV, except in a tiny region where the chargino is just slightly heavier than the sneutrino, which we neglect. We display as dashed lines in Fig. 1 contours of constant $m_{\tilde{\chi}^\pm} = 95$ and 100 GeV, the latter of which approximates the chargino mass reach of LEP200. The chargino bound cuts off most of the cosmological s-channel pole region. Light dotted contours indicate slepton bounds from searches for acoplanar lepton pairs at LEP183 and do not make inroads into the light shaded region. Constraints from Higgs searches are most severe at low $\tan\beta$, where the tree-level Higgs

mass $m_h \approx m_Z|\cos 2\beta|$ is smallest, and where the experimental lower bounds on the Higgs mass are strongest. The radiative corrections to the Higgs mass are large[27] and increase logarithmically with the stop masses; thus the Higgs mass bound may be satisfied for sufficiently large $m_{1/2}$, although such large values may be excluded from other, e.g. cosmological, considerations [13]. Higgs mass contours are shown as dot-dashed lines in Fig. 1. As $\tan\beta$ is increased, the tree-level Higgs mass grows, and additionally, the experimental lower bound on the Higgs mass falls; however, one becomes more susceptible to the upper bound on the Higgs mass from baryon asymmetry preservation, as above.

Supersymmetric particles could also contribute via loop effects to precision observables. Relevant constraints come, for instance, from the ρ parameter [28], which receives contributions when there is a mass difference between two members of an $SU(2)$ doublet. In the stop sector, the large top mass means that the doublet and singlet stops are in general mixed, i.e. the mass eigenstates are linear combinations of the doublet and singlet states, and so both mass eigenstates contribute to ρ. We need a light stop $m_{\tilde{t}_2} \sim m_t$ for electroweak baryogenesis; for this to be consistent with the determination of ρ, the light stop needs to be mostly singlet, and the doublet stop heavy enough. This happens for some parameters in the CMSSM because the RGEs run the soft singlet mass smaller than the doublet mass, and the doublet-singlet mixing will be small if $(A + \mu\cot\beta)$ is small. It is worth clarifying that the constraint from the ρ parameter depends on the amount of mixing. As the stop mixing angle increases from zero, the lower bound on the soft mass of the heavy squark ($\approx$ doublet) *decreases*, but for large enough mixing it increases again [29].

Another constraint on SUSY models is the decay $b \to s\gamma$, to which a light charged Higgs and/or a light chargino and squark can make substantial contributions [30]. For the area of parameter space we are interested in, the charged Higgs is moderately heavy (400 –700 GeV) but we certainly have a light stop. The contribution to the $b \to s\gamma$ amplitude from charged Higgs-top exchange in SUSY is always negative, as is the SM amplitude, and decreases in magnitude as m_{H^+} increases. The chargino-squark contributions are more complicated. If the up and charm squark masses are comparable to that of the doublet stop, as is the case for our parameters, then the charm squark-gaugino amplitude plus the up squark-gaugino amplitude will be of opposite sign to the stop-gaugino contribution (because of CKM unitarity) so the up and charm squarks can partially cancel the (heavy doublet) stop amplitude. The squarks also have Yukawa-strength interactions with the Higgsino component of the chargino, which are strong for the stops. This "stop-Higgsino" amplitude is proportional to the singlet-doublet stop mixing, which is small in the area of parameter space we are interested in. However, for our parameters, the sign of the stop-Higgsino amplitude is $-sgn(\mu)$. Since we take μ positive so as to cancel against A (which is negative in the regions of interest) in the stop mixing mass, we find that this remaining stop-chargino contribution is *negative* like the SM and charged Higgs amplitudes. This absence of cancellation between the SUSY contributions to $b \to s\gamma$ will make the branching ratios in our "allowed for DM and the BAU" region larger than in the SM, and potentially problematic.

3 Results

We now present our analysis of the regions of the CMSSM parameter space which satisfy the experimental and cosmological constraints outlined above. In all our numerics, we run the soft mass parameters and gauge and Yukawa couplings to the electroweak scale with two loop RGEs for the

couplings and gaugino masses and one-loop RGEs for other masses. In practice, we find that the stop mass constraint is the most difficult to satisfy. This is because the gluino contribution to the running of the stop mass^2 parameters in (5) tends to drive the light stop mass to values larger than that permitted by the preservation of the baryon asymmetry. The terms in (5) proportional to the top Yukawa coupling drive the stop masses down, and at fixed $m_{1/2}$ and m_0, we have the option of varying A_0 to help produce a light stop. We will see that this requires a fairly large and particular range of values for A_0. Of course, there is a similar term proportional to the tau Yukawa coupling in the RGE for the stau mass^2 parameters, and for some ranges of parameters at medium to large $\tan\beta$, the light stau mass^2 can be driven negative.

We now fix $\tan\beta = 12$ and $m_0 = 145\,\mathrm{GeV}$ and plot the combined set of experimental and theoretical constraints in the $(m_{1/2}, A_0)$ plane. As we're interested in the region where the doublet-singlet stop mixing angle is reasonably small, we concentrate here on the area of parameter space where the sign of μ is opposite to that of A, to allow cancellation in the off-diagonal elements of (4). Also, the presence of a quasi-fixed point for A_t at low $\tan\beta$ tends to drive A_t to positive values in the vicinity of $2m_{1/2}$[35], which tends to be much larger than $|\mu|\cot\beta$. Smaller $|A_t|$ can be generated at moderate $\tan\beta$ by taking A_0 large and negative. Accordingly, in Fig. 2a, we consider negative A_0 and positive μ. The light shaded region is excluded because it contains either a tachyonic stop or stau. The dashed contour combines the experimental bounds from chargino, stop and Higgs searches with the condition that the LSP be the neutralino, to avoid an excess of charged dark matter [25]. In particular, for the Higgs bound, we take 91 GeV at $\tan\beta = 4$ and 83 GeV at $\tan\beta = 6 - 12$ [36]. In Fig. 2a, the vertical left side of the dashed contour is due to the chargino bound, the diagonal piece which parallels the light shaded region is due to the stop bound, and the horizontal piece is the line $m_{\tilde{\chi}} = m_{\tilde{\tau}_R}$ [4]. The experimental Higgs constraint does not provide a useful bound for this value of $\tan\beta$. The solid line gives the BAU constraint: above the solid line, sphaleron processes wash out the baryon asymmetry, while below the solid line the baryon asymmetry is preserved. In the figures we present, the BAU boundary is typically set by the condition that the stop mass be sufficiently light. Lastly, the dark hatching marks the region where the neutralino relic density violates the cosmological upper bound $\Omega_{\widetilde{\chi}} h^2 \leq 0.3$. The region which is allowed by all of the experimental and cosmological constraints is then highlighted by diagonal shading. We show as the dotted line the lower boundary of the cosmologically preferred region, $\Omega_{\widetilde{\chi}} h^2 = 0.1$. Note that it bends away from the $m_{\tilde{\chi}} = m_{\tilde{\tau}_R}$ contour, as stau-neutralino coannihilation drives the relic abundance to small values for close stau-neutralino mass degeneracy. Notice also the chimney at $m_{1/2} \sim 110 - 130\,\mathrm{GeV}$, which is an analogous s-channel pole structure to that in Fig. 1.

In Figs. 3 and 4, we show the variation of BAU allowed region with m_0 and $\tan\beta$. In Fig. 3a and 3b, we've taken $m_0 = 135\,\mathrm{GeV}$ and $165\,\mathrm{GeV}$, respectively, for $\tan\beta = 12$. For $m_0 = 135\,\mathrm{GeV}$, the staus are lighter vis-a-vis the neutralinos, the horizontal piece of the dashed contour moves upward, and the combined chargino and LSP constraint almost wipe out the BAU allowed region entirely. Recall from Fig. 1 and the discussion in Section 2 that larger m_0 implies heavier sleptons, and a higher relic neutralino abundance, while lower m_0 implies a lower neutralino relic density. This is evident in Fig. 3a, where no contours of $\Omega_{\widetilde{\chi}} h^2 = 0.3$ are visible. In Fig. 3b, the staus are heavier vis-a-vis the neutralinos, and the combined experimental and BAU constraints permit a larger parameter region.

[4] We have not included the new preliminary bounds on the stau mass[24], which may slightly reduce the BAU allowed region.

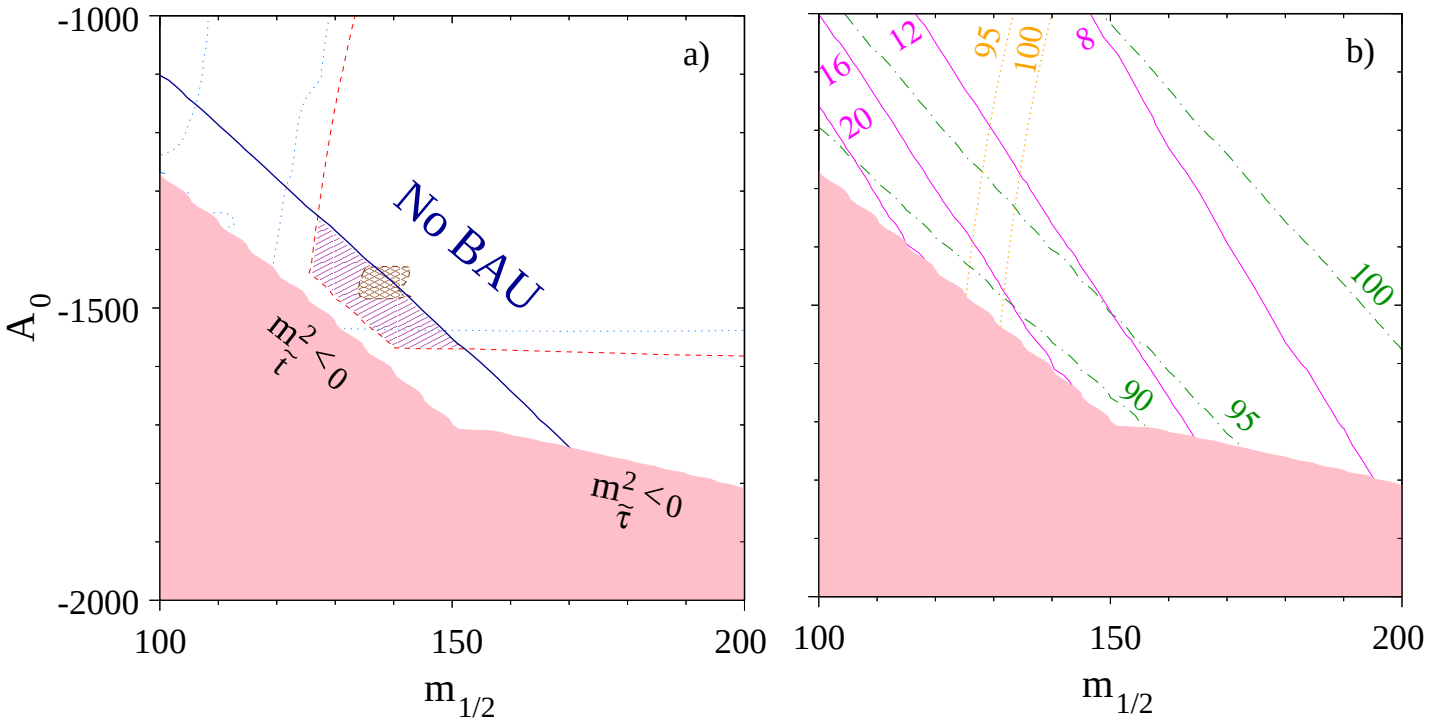

Figure 2: *In a), the region of mSUGRA parameter space satisfying the BAU, experimental and cosmological constraints described in the text, for* $\tan\beta = 12, m_0 = 145$ *GeV and* $\mu > 0$*, is marked by diagonal shading. Above the solid line, sphaleron processes wipe out the baryon asymmetry. The light shaded region contains tachyons. The dark hatched region has* $\Omega_{\tilde{\chi}} h^2 > 0.3$*. The dotted lines are contours of constant* $\Omega_{\tilde{\chi}} h^2 = 0.1$*. Contours of constant Higgs mass (dot-dashed), chargino mass (dotted) and* $\delta\rho \times 10^4$ *(solid) are displayed in b).*

However, here the relic densities are larger, and the constraint $\Omega_{\tilde{\chi}} h^2 < 0.3$ excludes the bulk of the BAU allowed region, leaving a small region near the line $m_{\tilde{\chi}} = m_{\tilde{\tau}_R}$, as above.

In Fig. 4, we show the BAU allowed regions for $\tan\beta = 6$ and 8, at $m_0 = 125\,\mathrm{GeV}$. Because the stau mass runs less for smaller $\tan\beta$, the horizontal piece of the dashed exclusion contour is moved to lower values of A_0, opening up more BAU allowed parameter space. One can also take a smaller m_0, so that the relic density constraint is easily satisfied. As in the case $\tan\beta = 12$, the allowed range of m_0 is limited on the low side by the requirement that the LSP be the neutralino, and on the high side by the relic density constraints. For $\tan\beta \leq 4$, the tighter experimental Higgs mass bound excludes the entire BAU allowed region. Overall, we find that the range $5 \lesssim \tan\beta \lesssim 12$ yields the largest BAU regions which satisfy the experimental and cosmological constraints. For simplicity, we've applied a single Higgs mass constraint (corresponding to large stop mixing) for all $m_{1/2}$ and A_0 at fixed $\tan\beta$. Of course in the BAU allowed regions, the stop mixing is in fact small, and the experiment bounds for $\tan\beta \leq 6$ are consequently tighter than those we have imposed and exclude all but a sliver of the BAU allowed region in Fig. 4a. The other figures are unaffected.

We emphasize that the signs of A_0 and μ were selected by the requirement that there be cancellations in the off-diagonal element of the stop mass matrix, leading to a small stop mixing angle.

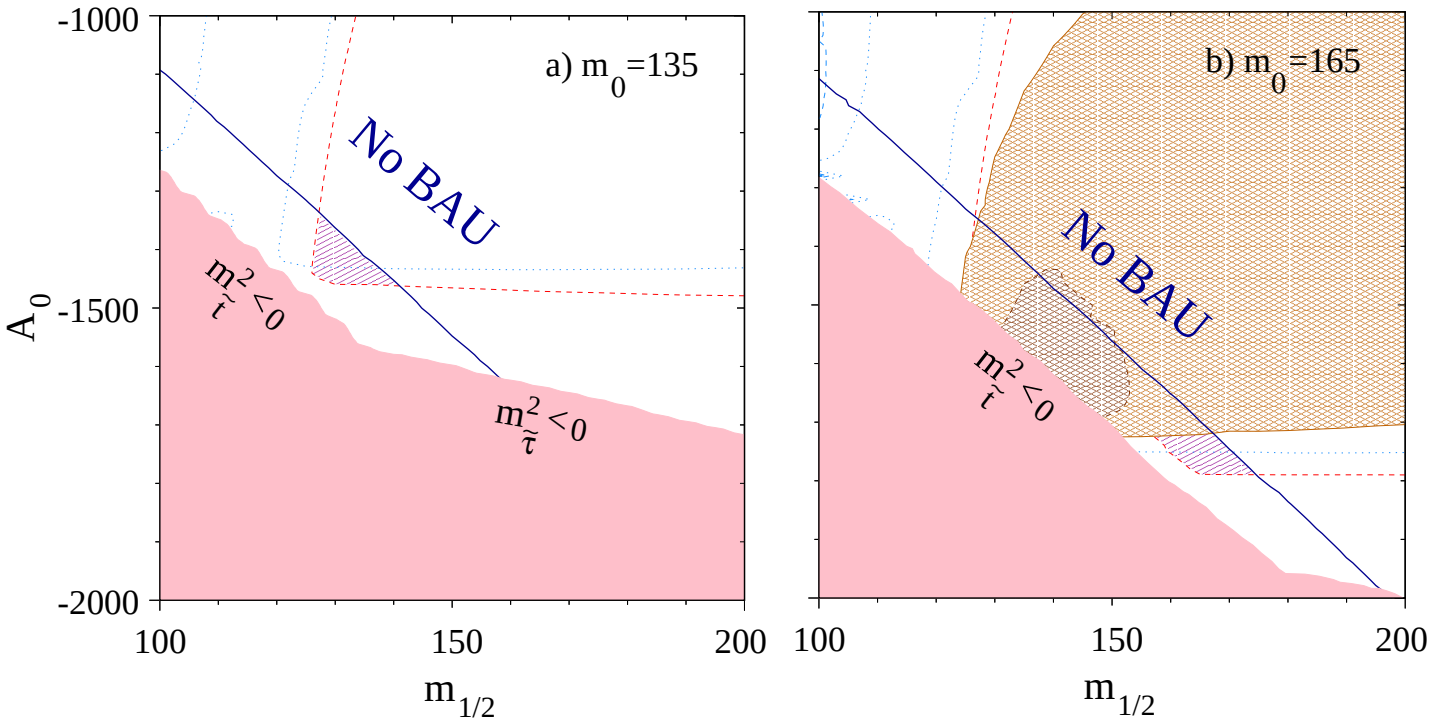

Figure 3: *The same as Fig. 2a, but for a)* $m_0 = 135\,\mathrm{GeV}$ *and b)* $m_0 = 165\,\mathrm{GeV}$. In b) the dark hatched region has $\Omega_{\tilde{\chi}} h^2 > 0.4$ and the light hatched region has $0.3 < \Omega_{\tilde{\chi}} h^2 < 0.4$.

This requires not only that A_t and μ have opposite signs, but also that $|A_t|$ be considerably below its quasi-fixed point value, which can only be achieved for A_0 large and negative. It is also possible to get small stop mixing for $\mu < 0$, since one can get small, positive A_t for large negative A_0. In fact, BAU regions do exist for $\mu < 0$, but they are considerably smaller even than the somewhat narrow allowed regions of Figs. 2-4.

We compute the one-loop stop contribution to $\Delta\rho$ from [28]. Contributions from other SUSY particles are not included on our plots; from [37] we expect the sleptons and "-inos" to give at most $\Delta\rho < 0.0009$. Following [28, 38], we would like the stop contribution to be less than the one-sigma error on ϵ_1, which is [39] 0.0012. All the supersymmetric contributions to $\Delta\rho$ should therefore fit comfortably within the two sigma error bars. In Fig. 2b, we show contours of constant $\Delta\rho$, along with chargino and Higgs mass contours, to demonstrate how the BAU allowed region will be further constrained by improved experimental bounds in the future. For this value of $\tan\beta$, the entire BAU region is already excluded by the requirement $\Delta\rho < 0.0012$. For $\tan\beta = 6$ and 8, by contrast, the entire BAU allowed regions have $\Delta\rho < 0.0010$ and 0.0012, respectively.

To estimate the $b \to s\gamma$ branching ratio for the parameter space we are interested in, we have calculated the LO contributions to $C_7(m_W)$ and $C_8(m_W)$ following [31], and the branching ratio from formulae in [33], who include NLO corrections in the running from m_W to m_b. The branching ratios we find are large :$BR \sim 4.1$—6.7×10^{-4}. CLEO measures $3.15 \pm 0.35 \pm 0.32 \pm 0.26 \times 10^{-4}$ [34]. If we impose the requirement that the branching ratio we calculate be smaller than the CLEO 95% C.L. measurement ($B.R. < 4.5 \times 10^{-4}$ [34]), then we find that the $\tan\beta = 6$ and 8 "allowed for

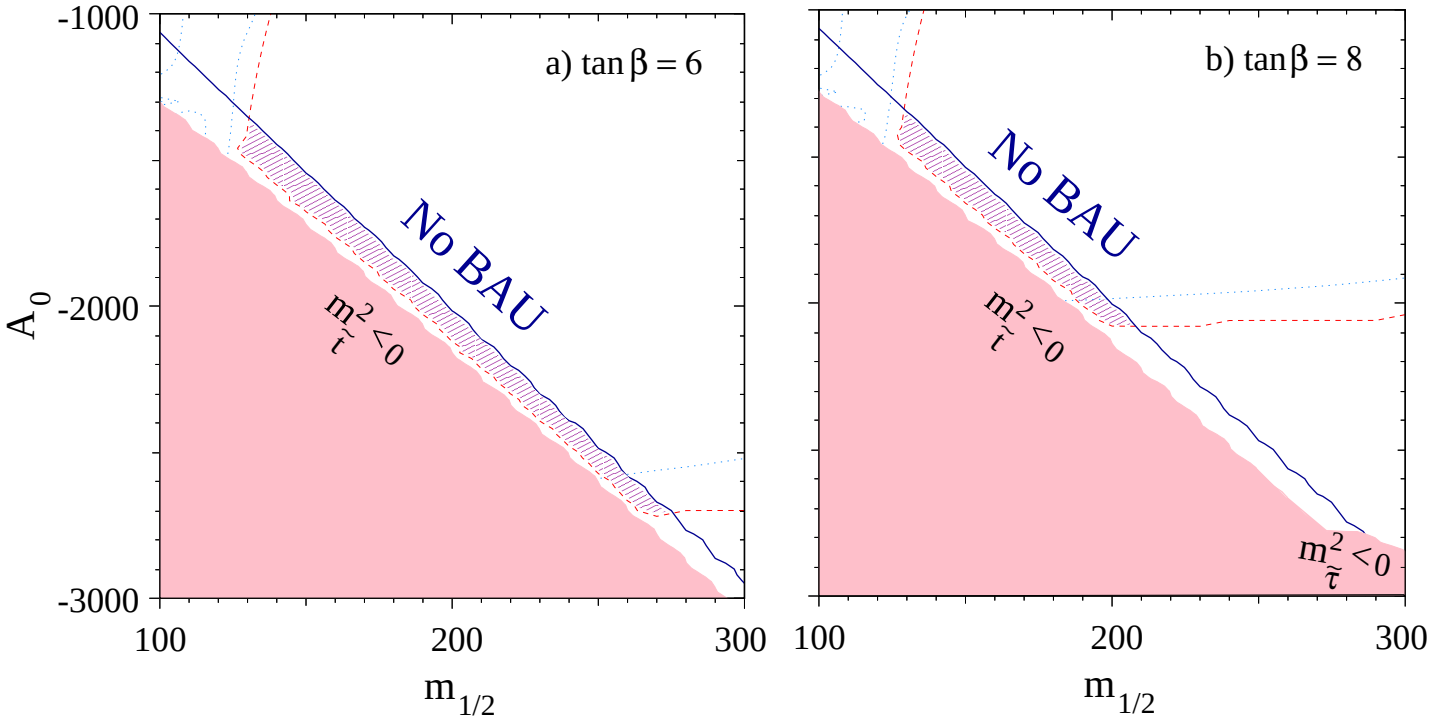

Figure 4: *The same as Fig. 2a, but for a)* $\tan\beta = 6$ *and b)* $\tan\beta = 8$. $\Omega_{\tilde{\chi}} h^2$ is less than 0.3 everywhere in the plots.

baryogenesis and dark matter" regions satisfy this requirement ($BR \sim 4 \times 10^{-4}$). However, over most of the $\tan\beta = 12$ region, we find branching ratios of order $6 - 7 \times 10^{-4}$, which is too large. The branching ratio is very sensitive to the charm and up squark masses, because these squarks contribute to $C_7(m_W)$ with the opposite sign from the stop, and so even a relatively small relaxation of the the CMSSM boundary conditions for the squarks can have a significant impact on the rate for $b \to s\gamma$. For instance, decreasing the charm squark mass by 100 GeV $(15 - 25\%)$ decreases the branching ratio we calculate below the CLEO 95% bound. A NLO [32] calculation would be required to reliably calculate $b \to s\gamma$ in our large $\tan\beta$ region, because the NLO corrections can be significant when there are cancellations between different contributions. In summary, although $BR(B \to X_s\gamma)$ is greater than in the Standard Model, it is not prohibitively large, at least for $\tan\beta = 6, 8$, because 1) the charged Higgs is moderately heavy, 2) the charm squark and gaugino partially cancel the stop and gaugino contribution, and 3) the stop and Higgsino contribution is proportional to the stop mixing, which is small.

Lastly, we note that if a Higgs is not observed at LEP200, the increased Higgs mass bounds will exclude most of the remaining BAU allowed parameters space in the CMSSM. If any BAU region remains, it will be at large $\tan\beta \gtrsim 10$, where the Higgs bound can fall below ~ 95GeV. The BAU allowed regions in Figs.4 have Higgs masses between $\sim 88 - 92$ GeV and will be forbidden if the Higgs is not seen before the end of LEP running.

4 Conclusions

In the CMSSM, we have found the area of parameter space consistent with present experimental limits which predicts a neutralino relic density $0.1 \lesssim \Omega h^2 \lesssim 0.3$, and where sphaleron processes do not wipe out the Baryon Asymmetry of the Universe. The allowed regions correspond to large $|A_0|$, because this ensures that the RH stop soft mass is small, as required by the baryogenesis constraint. They also occur for negative A_0 and positive μ, because this allows cancellations between μ and A in the off-diagonal elements of the squark mass matrix (4), which is dictated by baryogenesis, as well. There also exist allowed regions at negative A_0 and negative μ, but these are quite tiny, even compared to the small regions we find for positive μ. We find that the current Higgs mass constraints exclude all BAU allowed regions for $\tan\beta \lesssim 5$, and for $\tan\beta \gtrsim 12$, the BAU allowed regions become very constrained. We find the branching ratio for $b \to s\gamma$ in the allowed regions to be larger than the SM, but consistent with present CLEO data for smaller values of $\tan\beta$. Lastly, we find that if LEP200 should not find a Higgs, almost all of the currently BAU allowed regions will be excluded, with the possible exception of those at the largest $\tan\beta$, where the Higgs mass bounds will be weakest.

Acknowledgments S.D. would like to thank Paolo Gambino for clear explanations, and Steve Abel and Gian Giudice for useful conversations. The work of T.F. was supported in part by DOE grant DE–FG02–95ER–40896, and in part by the University of Wisconsin Research Committee with funds granted by the Wisconsin Alumni Research Foundation.

References

[1] For a review of particle candidates and detection schemes, see *e.g.* G. Jungman, M. Kamionkowski, K. Greist, *Phys. Rep.* **267** (1996) 195, and references therein.

[2] for a review, see *e.g.*
V.A. Rubakov, M.E. Shaposhnikov, *Physics-Uspekhi* **39** (1996) 461.
A. Cohen, D.B. Kaplan, and A.E. Nelson. *Annu. Rev. Nucl. Part. Sci.*, 43:27, 1993.
M. Quiros. *Helv. Phys. Acta*, 67:451, 1994.
A. Riotto. Technical Report (hep-ph/9807454), 1998.

[3] for a review, see *e.g.*
H. Dreiner, in *Perspectives on Supersymmetry*, Ed. by G.L. Kane, World Scientific, hep-ph/9707435;
G. Bhattacharyya, *Nucl. Phys. Proc. Suppl.* **52A** (1997) 83, hep-ph/9608415.

[4] A.D. Sakharov, *JETP Lett.* **5** (1967) 24.

[5] G.Farrar and M. Shaposhnikov, *Phys. Rev. Lett.* 2833 (1993); (E) **71** 210 1993.

[6] M.B. Gavela, P. Hernandez, J. Orloff, O. Pène and C. Quimbay, *Mod. Phys. Lett.* **9** 795 1994.

[7] V.A. Kuzmin, V.A. Rubakov, and M.E. Shaposhnikov. *Phys. Lett.*, B155:36, 1985.

[8] K. Kajantie, M. Laine, K. Rummukainen, M. Shaposhnikov, *Nucl.Phys.* **B466** (1996) 189.

[9] M. Losada. *Phys. Rev.*, **56** 2893, 1997.
M. Laine. *Nucl. Phys.*, **B481** 43, 1996.

[10] M. Carena, M. Quiros, C.E.M. Wagner, *Nucl.Phys.* **B524** (1998) 3 ; hep-ph/9710401

[11] M. Laine, K. Rummukainen, *Nucl.Phys.* bf B535 (1998) 423; hep-lat/9804019

[12] M. Losada, *Nucl. Phys.* **B537** (1999) 3.
M. Losada, (hep-ph/9905441) 1999.

[13] J. Ellis, T. Falk, K.A. Olive and M. Schmitt, Phys. Lett. **B388** (1996) 97; J. Ellis, T. Falk, K.A. Olive and M. Schmitt, Phys. Lett. **B413** (1997) 355; J. Ellis, T. Falk, G. Ganis, K.A. Olive and M. Schmitt, Phys. Rev. **D58** (1998) 095002.

[14] S. Myint, *Phys. Lett.* **B287** (1992) 325. G.Giudice, *Phys. Rev.* **D45** (1992) 3177. J.R. Espinosa, M. Quiros, F. Zwirner, *Phys. Lett* **B307** (1993) 106, Brignole *et al., Phys. Lett.* **B324** (1994) 181, M. Carena, M. Quiros, C. Wagner *Phys. Lett.* **B380** (1996) 81. D. Delepine *et al., Phys. Lett.* **B386** (1996) 183.

[15] M.E. Shaposhnikov. *Nucl. Phys.*, B287:757, 1987.

[16] J.R. Espinosa, *Nucl. Phys.* **B475** (1996) 273.

[17] see *e.g.*, P. Arnold, O. Espinosa, *Phys. Rev.* **D47** (1993) 3546.

[18] M. Dine, R. G. Leigh, P. Huet, A. Linde, D. Linde, *Phys.Rev.* **D46** (1992) 550.

[19] K. Kajantie, M. Laine, K. Rummukainen, M. Shaposhnikov, *Nucl.Phys.* **B458** (1996) 90; hep-ph/9508379.

[20] D. Bodeker, P. John, M. Laine, and M.G. Schmidt. *Nucl. Phys.*, B497:387, 1997.

[21] J. Cline, G.D. Moore, and G. Servant. Technical Report (hep-ph/9902220), 1999.

[22] W. de Boer *et al.*, *Z.Phys.* **C71** (1996) 415.

[23] S.A. Abel, Ben Allanach *Phys.Lett.* **B415** (1997) 371; hep-ph/9707436. P. Brax, C.A. Savoy, *Nucl. Phys.* **B447** (1995) 227.

[24] Official compilations of LEP limits on supersymmetric particles are available from:
`http://www.cern.ch/LEPSUSY/`;
for an official compilation of LEP Higgs limits, see:
The LEP Working Group for Higgs Boson Searches, ALEPH, DELPHI, L3 and OPAL, CERN-EP/99-060.

[25] J. Ellis, J.S. Hagelin, D.V. Nanopoulos, K.A. Olive and M. Srednicki, Nucl. Phys. **B238** (1984) 453.

[26] J. Ellis, T. Falk, and K.A. Olive, Phys. Lett. **B444** (1998) 367.
J. Ellis, T. Falk, K.A. Olive, and Mark Srednicki, hep-ph/9905481.

[27] H.E. Haber, R. Hempfling and A.H. Hoang, Zeit. für Phys. **C75** (1997) 539; M. Carena, M. Quiros and C.E.M. Wagner, Nucl. Phys. **B461** (1996) 407; S. Heinemeyer, W. Hollik and G. Weiglein, Phys. Rev. **D58** (1998) 091701; R. Zhang, Phys. Lett. **B447** (1999) 89; and references therein.

[28] A. Djouadi, P. Gambino, S. Heinemeyer, W. Hollik, C. Junger, G. Weiglein, *Phys.Rev.* **D57** (1998) 4179; hep-ph/9710438

[29] M. Carena, P.H. Chankowski, S. Pokorski, C.E.M. Wagner, *Phys.Lett.* **B441** (1998) 205; hep-ph/9805349.

[30] for a review, see *e.g.*
M. Misiak, S. Pokorski, J Rosiek, *Heavy Flavours II* eds. A.J. Buras, M. Lindner, World Scientific, Singapore; hep-ph/9703442.

[31] R. Barbieri, G.F. Giudice, *Phys.Lett.* **B309** (1993) 86; S. Bertolini, F. Borzumati, A. Masiero, G. Ridolfi, *Nucl.Phys.* **B353** (1991) 591, P. Cho, M. Misiak, D. Wyler, *Phys.Rev.* **D54** (1996) 3329.

[32] M. Ciuchini, G. Degrassi, P. Gambino, G.F. Giudice, *Nucl.Phys.* **B534** (1998) 3.

[33] A.L. Kagan, M. Neubert, *Eur.Phys.J.* **C7** (1999) 5; hep-ph/9805303.

[34] CLEO Collaboration at ICHEP98, CLEO CONF 98-17.

[35] M. Carena , M. Olechowski , S. Pokorski and C.E.M. Wagner, Nucl.Phys. **B426** (1994) 269 and references therein.

[36] The DELPHI Collaboration, DELPHI 99-8 CONF 208.

[37] P. Chankowski *et.al.*, *Nucl. Phys.* **B417** (1994) 101.

[38] G. Altarelli, XVIII Int. Symp. on Lepton-Photon Interactions, Hamburg 1997.

[39] C. Caso *et al. Eur. Phys. J.* **C3** (1998) 1.